Naval Research Laboratory

Washington, DC 20375-5320

NRL/MR/5652--07-9061

Analysis of an Optical Channelization Technique for Microwave Applications

MATTHEW S. ROGGE
VINCENT J. URICK
FRANK BUCHOLTZ

Photonics Technology Branch
Optical Sciences Division

June 27, 2007

REPORT DOCUMENTATION PAGE

Form Approved
OMB No. 0704-0188

1. REPORT DATE *(DD-MM-YYYY)*	**2. REPORT TYPE**	**3. DATES COVERED** *(From - To)*
27-06-2007	Memorandum Report	01-01-2005 – 19-07-2005

4. TITLE AND SUBTITLE

Analysis of an Optical Channelization Technique for Microwave Applications

5a. CONTRACT NUMBER

5b. GRANT NUMBER

5c. PROGRAM ELEMENT NUMBER

6. AUTHOR(S)

Matthew S. Rogge,* Vincent J. Urick, and Frank Bucholtz

5d. PROJECT NUMBER

5e. TASK NUMBER

5f. WORK UNIT NUMBER

7. PERFORMING ORGANIZATION NAME(S) AND ADDRESS(ES)

Naval Research Laboratory, Code 5652
4555 Overlook Avenue, SW
Washington, DC 20375-5320

8. PERFORMING ORGANIZATION REPORT NUMBER

NRL/MR/5652--07-9061

9. SPONSORING / MONITORING AGENCY NAME(S) AND ADDRESS(ES)

Office of Naval Research
One Liberty Center
875 North Randolph Street
Arlington, VA 22203-1995

10. SPONSOR / MONITOR'S ACRONYM(S)

ONR

11. SPONSOR / MONITOR'S REPORT NUMBER(S)

12. DISTRIBUTION / AVAILABILITY STATEMENT

Approved for public release; distribution is unlimited.

13. SUPPLEMENTARY NOTES

*Presently with Quest L.L.C., Wellington, MO

14. ABSTRACT

Increasing electrical bandwidth combined with improved optical filtering allow for a new class of optical channelizers for use in RF, microwave, and millimeter-wave applications. After a brief refiew of existing channelization technology, an optical channelizer that uses optical local oscillators and optical filters is analyzed. Linearity and other limitations of the scheme show a strong dependence on the linearity of the optical modulator. The optical modulator is explored in both the optical domain and in the electrical domain. For the channelizer, it is shown that consideration must be given to nonlinearities in the optical field itself.

15. SUBJECT TERMS

Analog photonics
Microwave photonics
Optical channelization

16. SECURITY CLASSIFICATION OF:			**17. LIMITATION OF ABSTRACT**	**18. NUMBER OF PAGES**	**19a. NAME OF RESPONSIBLE PERSON**
					Vincent J. Urick
a. REPORT	**b. ABSTRACT**	**c. THIS PAGE**	UL	18	**19b. TELEPHONE NUMBER** *(include area code)*
Unclassified	Unclassified	Unclassified			(202) 767-9352

TABLE OF CONTENTS

ANALYSIS OF AN OPTICAL CHANNELIZATION TECHNIQUE FOR MICROWAVE APPLICATIONS

EXECUTIVE SUMMARY

- A brief review of channelization technologies is given.
- The impact of electro-optic modulator nonlinearities on an optical channelizer is explained in detail.
- An optical channelization technique is presented and analyzed, demonstrating a spurious-free dynamic range of 105 $dB \cdot Hz^{2/3}$.
- The nonlinearities introduced by electro-optic modulators, particularly in the optical domain, must be mitigated in high-performance optical channelizers.

Manuscript approved May 21, 2007.

ANALYSIS OF AN OPTICAL CHANNELIZATION TECHNIQUE FOR MICROWAVE APPLICATIONS

1 INTRODUCTION

Channelization is a common RF technique for wideband receivers [1]. In frequency-based channelization, the received signal is divided into narrow frequency bands, or channels, typically with RF filters. The quality of the channelization ultimately determines the performance. Several electrical filtering techniques and the acousto-optic Bragg cell have previously been proposed and developed to perform the channelization. Early acousto-optic channelizers for communications and radar applications suffered from inefficiency and power limitations. Recent developments in ultra-narrow, multiple-channel optical filters may provide new opportunities for optical channelizer technology. In particular, the capability to channelize the large bandwidths afforded by optical systems into RF-size frequency bins will offer significant improvements in signal processing tasks.

A brief overview of channelizer technology and the basic operation of an optical channelizer based on optical filtering are described in Section 2. A more detailed analysis of the system shows the importance of the optical modulator and demonstrates the need to consider the optical field. Since the optical channelizer directs only a portion of the optical spectrum onto the photodetector in each channel, spurious field components generated by the modulator that may otherwise cancel at the photodetector must be considered. Ideally, the optical modulator should be linear in the optical electric field, a much more stringent requirement than traditional microwave photonic links which require linearity only in the post-detection RF photocurrent. Such a modulator does not exist today.

Section 3 discusses the linearity limits set by the optical modulator for both a traditional electrooptic Mach-Zehnder interferometric intensity modulator (MZM) and an electrooptic phase modulator (ΦM). For the MZM, linearity in both the electrical domain (after the photodetector) and the optical domain (as seen at the output of the MZM) are reviewed. Section 4 explores the impact of nonlinearities in the optical field on the optical channelizer using a simple experimental setup. The work is summarized in Section 5.

2 OPTICAL CHANNELIZER OVERVIEW

A thorough review of existing channelization technology is presented in [1] (and the references therein). This work focuses on frequency-based channelization, in which the received signal is divided into narrow frequency channels. Each channel is then detected with a relatively narrowband receiver. The reduced noise bandwidth and any processing gain in the receiver (theoretically) allow for improved sensitivity. If the hardware is repeated for each channel, the result can be a wideband receiver whose sensitivity approaches that found in a narrowband receiver. Other benefits of channelized receivers include the ability to intercept several time-coincident signals without loss of information, potentially higher probability of intercept (POI), and higher signal throughput rates owing to the parallel architecture.

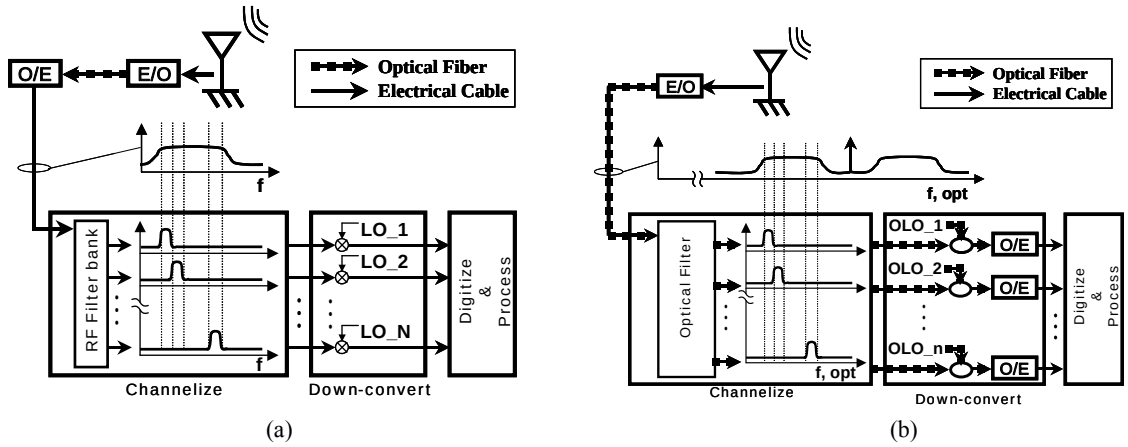

Fig. 1. A traditional digitizing RF channelizer with microwave photonic link extension is shown in (a). The antenna receives the RF signal, which is applied to an optical modulator for the electrical-to-optical conversion (E/O). After traveling on fiber to the processing station, a photodetector performs the optical-to-electrical (O/E) conversion and the spectrum of the photocurrent is shown. The rest of the channelizer, including the local oscillators (LO) is electronic. Electrical spectra both before and after the channelization are shown. The optical channelizer shown in (b) performs more functions in the optical domain, such as channelization and down-conversion. The optical local oscillators (OLO) are optical carriers at the appropriate frequency for down-conversion. The optical spectra both before and after channelization are shown in the figure.

A generic, fully populated RF channelized system is shown in Fig. 1(a). The channelization, down-conversion, digitization, and processing all occur in the electrical domain. Note that for a system with hundreds of channels, the size/weight/power demands of a fully populated receiver are usually not practical. Indeed, systems that switch different bands (groups of channels) onto a channelizer are more common in practice. Figure 1 assumes that the conditions between the receiver and the processing station are severe enough (e.g. far enough apart or electrically noisy) that a microwave photonic link is preferred. Hence, in Fig. 1(a) photonics plays the role of "RF link extender". The RF spectrum of the received signal is shown both before and after channelization.

Photonics assumes much more functionality in Fig. 1(b), which shows an optically channelized microwave photonic system with similar functionality. Notice the channelization and down-conversion occur in the optical domain by means of narrow optical filters and photodetectors, respectively. In this case, the optical spectrum is shown after the optical modulator and after the optical channelizing filter. The optical spectrum before the filter is double sideband. The filter need only channelize one of the sidebands, blocking the other.

The architecture depicted in Fig. 1(b) is significantly different from the first generation acousto-optic (AO) channelizers [2]. Acousto-optic channelizers pass coherent light through an acoustic Bragg cell onto an array of photodetectors. The received signal is applied to the acoustic transducer. The acoustic wave in the Bragg cell deflects the incident light an amount determined by the frequency of the applied signal. Typically, the AO transducer requires considerably high drive voltages. The new architecture in Fig. 1(b) assumes passive optical filtering technology will perform the channelization. As a result, traditional modulators handle the electrical-to-optical conversion with significantly higher bandwidth and efficiency. Many limits set by AO technology are completely avoided in the proposed architecture.

For sufficiently wideband receivers (i.e. many channels), the size/weight/power benefits of an optically channelized system can be significant. For example, an array of N photodetectors down-converts all the channels in the optical system whereas N mixers are required for the electrical

channelization system. Additionally, optical comb generators and the appropriate filter could potentially provide a low-power, compact array of optical local oscillators. If total system bandwidths exceed tens of GHz, the cost and power of electrical components (e.g. filters, combiners, local oscillators) becomes increasingly high. All-electronic millimeter-wave systems face serious implementation and realization challenges.

Importantly, the optically channelized system operates directly on the optical spectrum. Just as the performance of electrical channelizers depends on the RF filter, the frequency response of the optical filter plays a critical role in the optical channelizer. The filter is passive and interferometric in nature, so amplitude and phase distortion are a concern, but linearity should be preserved. Good out-of-band suppression and a flat pass band are required. If the filter is cyclic, for example, portions of the upper and lower sideband as well as higher order nonlinearities may wrap around and fall into the same channel. Depending on the system design (e.g. placement of the local oscillator), some of these extra components can be filtered in the RF domain. Much like a traditional channelizer, the optical filter will face ambiguity challenges when the frequency of the signal lies near the boundary of two channels.

Ideally, the filter allows only the portion of the optical spectrum containing the channel of interest to exit through a particular output port. Current state-of-the-art multi-channel optical filters are pushing below 12.5-GHz channel spacing (e.g. Essex Corporation Hyperfine WDM [3]), with theory allowing sub-GHz channelization [4]. Out of band optical suppression of greater than 40 dB is currently achievable, but ultimately 60 dB or more is preferred and theoretically possible.

Another important subsystem is the optical local oscillator (OLO) generation. Figure 1(b) only describes the basic architecture and operation. The mechanism by which the optical local oscillators are generated and even how they are combined with the received signal remain considerable design challenges. In general, each photodetector should receive a portion of signal bandwidth and an OLO that is spaced at the designed intermediate frequency (IF). Depending on the purpose of the channelizer (e.g. signal detection or frequency analysis), the OLO may have to be phase-locked to the original optical carrier. While Fig. 1(b) shows independent OLOs joining their respective channel after the filter, this need not be the case. With the appropriate filter, for example, a comb of OLOs could enter the channelizer filter alongside the data spectrum and be routed to the appropriate output. Mode-locked lasers are popular candidates for generating an OLO comb [5]-[7], although other solutions may ultimately prove more reliable [8],[9].

Clearly, the optical channelizer depends on significant advances along several fronts in optical device technology. In both Fig. 1(a) and (b), the electrical-to-optical conversion (i.e. the modulator) produces nonlinearities that can limit the overall performance of the system. Note that in Fig. 1(a) the entire optical spectrum from the modulator reaches the photodetector, so the traditional RF photocurrent equations for link linearity and performance directly apply. The performance and RF photocurrent for the optical channelizer of Fig. 1(b), on the other hand, depends entirely on what portion of the optical spectrum exits the filter in that channel and the strength and frequency of the optical local oscillator. In order to analyze the optical channelizer, one must consider the optical field exiting the modulator.

3 NONLINEARITY DUE TO THE OPTICAL MODULATOR

The Mach-Zehnder modulator (MZM) has long been the external modulator of choice for microwave photonic links [10]. Although not linear, the MZM behaves predictably and has been thoroughly evaluated. Phase modulators (ΦMs) use the same electrooptic effect in a single path

device, but when the entire output spectrum is directed onto a photodetector, the RF photocurrent is zero. Since the optical channelizer suppresses one of the sidebands and passes only a portion of the optical spectrum, RF photocurrent can be produced using a ΦM and a ΦM should be considered as well. Finally, electro-absorption modulators (EAM) should be considered for their potentially small size, weight, and drive voltage. The next subsection evaluates the MZM, followed by subsections briefly discussing both ΦM and EAM.

3.1 Optical Field from a Mach-Zehnder Modulator

The nonlinearity of the MZM in terms of RF photocurrent from a photonic link is well understood [11]-[15]. In the optical channelizer, however, the equations for RF photocurrent do not apply. Instead, we must consider the optical field exiting the MZM. Then, we can calculate the RF photocurrent and resulting nonlinearity based on what portion of that optical spectrum reaches a given photodetector.

We model the MZM as an ideal, balanced device and apply a complex exponential to its input,

$$\begin{bmatrix} E_{\text{out1}} \\ E_{\text{out2}} \end{bmatrix} = \underbrace{\frac{1}{2}\begin{bmatrix} 1 & j \\ j & 1 \end{bmatrix}\begin{bmatrix} e^{j\frac{\phi(t)}{2}} & 0 \\ 0 & e^{-j\frac{\phi(t)}{2}} \end{bmatrix}\begin{bmatrix} 1 & j \\ j & 1 \end{bmatrix}}_{MZM:\ splitter,\ phase\ shifters,\ combiner} \underbrace{\begin{bmatrix} E_0 e^{j\omega_0 t} \\ 0 \end{bmatrix}}_{input}, \tag{1}$$

where $\phi(t)$ is the phase change induced by the voltage applied to the modulator, $E_0 = \sqrt{\eta P_0}$ is the optical field amplitude, and ω_0 is the angular frequency of the optical carrier.

In this analysis, we apply two sinusoids of different frequencies to the MZM, so $\phi(t)$ is of the form

$$\phi(t) = \Gamma_0 + \frac{\pi}{V_\pi}\left(v_1 \sin\omega_1 t + v_2 \sin\omega_2 t\right), \tag{2}$$

where Γ_0 is the phase change due to the bias voltage, v_1 and v_2 are the amplitudes of the voltages applied to the modulator for tones at angular frequencies ω_1 and ω_2, respectively, and V_π is the on-off switching voltage. Equation (2) uses the same form as [11] to simplify comparison. The matrix in (1) that accounts for the phase shift $\phi(t)$ conveniently describes the fundamental problem of a MZM – the inherently nonlinear exponential modulation occurring in the branches of the interferometer.

Carrying out the calculation of (1) and simplifying leads to a result that contains the amplitude, phase, and frequency of the optical field components for one of the MZM outputs

$$E_{\text{out1}} = \begin{cases} jE_0 J_n\left(\frac{\pi v_1}{2V_\pi}\right) J_m\left(\frac{\pi v_2}{2V_\pi}\right) e^{j(\omega_0 + n\omega_1 + m\omega_2)t} \sin\left(\frac{\Gamma_0}{2}\right), \\ \qquad\qquad n+m,\ even \\ E_0 J_n\left(\frac{\pi v_1}{2V_\pi}\right) J_m\left(\frac{\pi v_2}{2V_\pi}\right) e^{j(\omega_0 + n\omega_1 + m\omega_2)t} \cos\left(\frac{\Gamma_0}{2}\right), \\ \qquad\qquad n+m,\ odd \end{cases}, \tag{3}$$
$$n, m = \ldots, -1, 0, 1, 2, \ldots$$

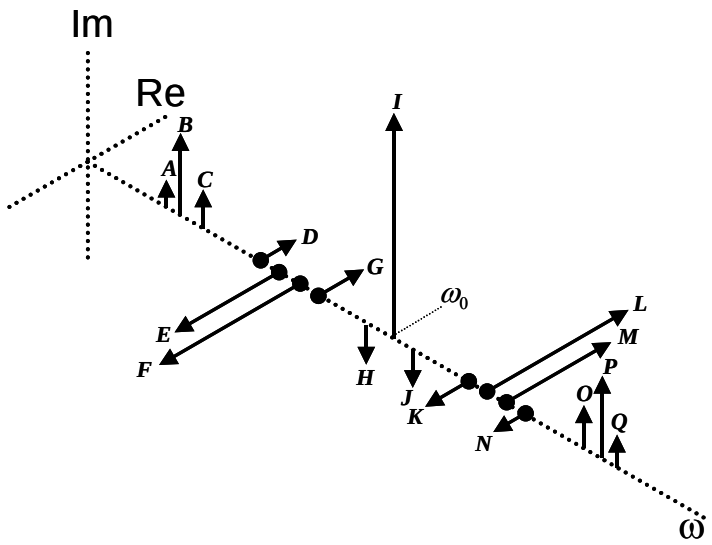

Fig. 2. Several of the most significant optical field components resulting from two-tone modulation on a balanced Mach-Zehnder modulator. Each term can be thought of as a phasor at its optical frequency. The optical carrier is shown at Label I. Labels F & L and E & M are due to the fundamental RF tones applied at ω_1 and ω_2, respectively, with amplitudes $v_1 > v_2$ for illustrative purposes. Table I lists the amplitude, phase, and frequency for each labeled component. The components with solid dots at their base are odd order terms. When biased at a null, only odd order terms remain in the optical field.

where J_k is the k^{th} order Bessel function of the first kind. We use complex exponentials to readily see the double-sided optical spectrum. Figure 2 illustrates a portion of the optical spectrum for a MZM biased at quadrature (note that $J_{-n}(x) = (-1)^n J_n(x)$). Biasing at quadrature ($\Gamma_0 = \pi/2$) sets the amplitude scaling due to the bias equal for both odd and even order harmonics, since $\cos(\pi/4) = \sin(\pi/4)$. Assuming moderate to small modulation depth, only the most significant terms are shown and labeled in the figure. The amplitude, phase, and optical frequency of the labeled components are summarized in Table I.

An ideal optical spectrum analyzer (OSA) would show the power (field-magnitude-squared) of each component in (3). Figure 3 plots the OSA spectrum taken on an ANDO AQ6319 OSA for two +5 dBm RF tones applied to a MZM ($V_\pi \approx 5$ V) biased at quadrature. The laser-only spectrum is also shown to illustrate the spectral limitation set by the OSA, and each of the components from Fig. 2 and Table I are labeled as well. Note that significant second order harmonics are present in the optical field for a MZM biased at quadrature.

Careful examination of (3) indicates that biasing the modulator at a null ($\Gamma_0 = 0$) will suppress all even order terms in the optical field, including the carrier ($\sin(\Gamma_0) = 0$). In addition, the fundamental and odd order harmonic amplitudes are maximized for a given drive voltage ($\cos(\Gamma_0) = 1$). Carrier suppression in the optical channelizer is not an issue since it is assumed that optical local oscillators will be added to the channelizer outputs prior to photodetection. The difference between the optical spectra for quadrature-bias and null-bias is appreciable. All the components shown in Fig. 2 are present at quadrature while only those with solid dots at their base exist at null bias. The amplitudes of the odd order harmonics also increase by a factor of $\sqrt{2}$ at null compared to quadrature.

TABLE I
SUMMARY OF DOMINANT OPTICAL FIELD COMPONENTS EXITING A MZM BIASED AT QUADRATURE WITH TWO RF TONES APPLIED

Fig. 1 Label	Optical Frequency	Amplitude	Phase	Index in Eq. 3	
				n	*m*
A	$\omega_0-2\omega_2$	$E_0J_0(A_1)J_2(A_2)/\sqrt{2}$	π/2	0	-2
B	$\omega_0-\omega_1-\omega_2$	$E_0J_1(A_1)J_1(A_2)/\sqrt{2}$	π/2	-1	-1
C	$\omega_0-2\omega_1$	$E_0J_2(A_1)J_0(A_2)/\sqrt{2}$	π/2	-2	0
D	$\omega_0-2\omega_2+\omega_1$	$E_0J_1(A_1)J_2(A_2)/\sqrt{2}$	0	1	-2
E	$\omega_0-\omega_2$	$E_0J_0(A_1)J_1(A_2)/\sqrt{2}$	π	0	-1
F	$\omega_0-\omega_1$	$E_0J_1(A_1)J_0(A_2)/\sqrt{2}$	π	-1	0
G	$\omega_0-2\omega_1+\omega_2$	$E_0J_2(A_1)J_1(A_2)/\sqrt{2}$	0	-2	1
H	$\omega_0+\omega_1-\omega_2$	$E_0J_1(A_1)J_1(A_2)/\sqrt{2}$	-π/2	1	-1
I	ω_0	$E_0J_0(A_1)J_0(A_2)/\sqrt{2}$	π/2	0	0
J	$\omega_0+\omega_2-\omega_1$	$E_0J_1(A_1)J_1(A_2)/\sqrt{2}$	-π/2	-1	1
K	$\omega_0+2\omega_1-\omega_2$	$E_0J_2(A_1)J_1(A_2)/\sqrt{2}$	π	2	-1
L	$\omega_0+\omega_1$	$E_0J_1(A_1)J_0(A_2)/\sqrt{2}$	0	1	0
M	$\omega_0+\omega_2$	$E_0J_0(A_1)J_1(A_2)/\sqrt{2}$	0	0	1
N	$\omega_0+2\omega_2-\omega_1$	$E_0J_1(A_1)J_2(A_2)/\sqrt{2}$	π	-1	2
O	$\omega_0+2\omega_1$	$E_0J_2(A_1)J_0(A_2)/\sqrt{2}$	π/2	2	0
P	$\omega_0+\omega_1+\omega_2$	$E_0J_1(A_1)J_1(A_2)/\sqrt{2}$	π/2	1	1
Q	$\omega_0+2\omega_2$	$E_0J_0(A_1)J_2(A_2)/\sqrt{2}$	π/2	0	2

The RF tones applied to the modulator have angular frequencies of ω_1 and ω_2. $A_1=\pi v_1/2V_\pi$ and $A_2=\pi v_2/2V_\pi$ (See Eq. (2)).

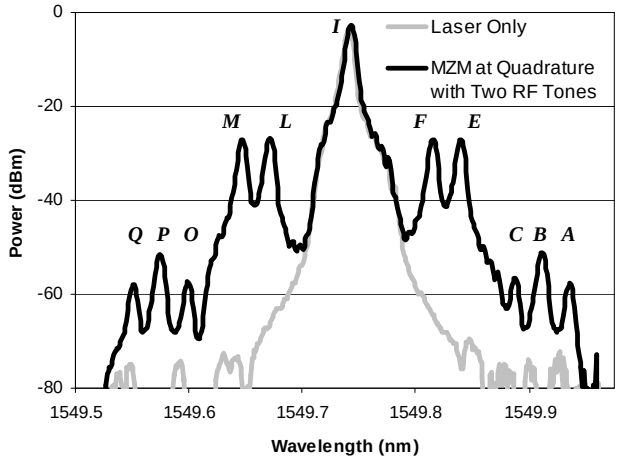

Fig. 3. Optical spectrum analyzer (OSA) plot of a MZM-modulated optical carrier where +5 dBm RF tones at 9 GHz and 12 GHz were applied to the MZM biased at quadrature. The labels applied to this plot correspond to Fig. 2 and Table I assuming $\omega_1=2\pi 9$ GHz and $\omega_2=2\pi 12$ GHz. The laser-only spectrum illustrates the limitation set by the OSA.

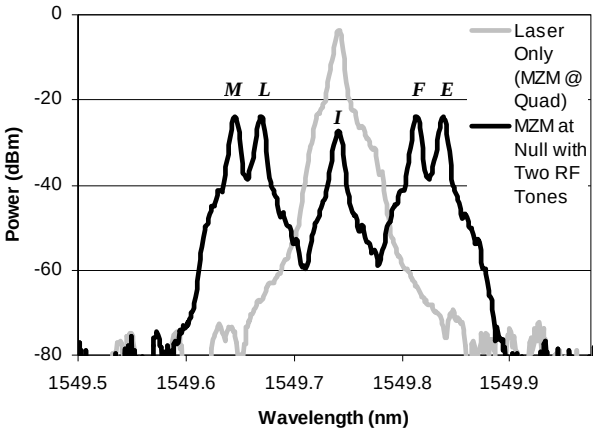

Fig. 4. Optical spectrum analyzer (OSA) plot of a MZM biased at a null with two +5 dBm RF tones at 9 GHz and 12 GHz applied. The labels correspond only to the frequencies in Fig. 2 and Table I assuming $\omega_1=2\pi\cdot 9$ GHz and $\omega_2=2\pi\cdot 12$ GHz. The laser-only spectrum shows an un-modulated MZM biased at quadrature to illustrate the amount of carrier suppression provided by the MZM bias.

Importantly, the dependence on modulator bias described in (3) only applies for a balanced MZM. The phase modulation inside the branch of the MZM always creates both even and odd order terms. The bias state, in conjunction with the combiner that follows the phase modulator, determines which optical field components exit a particular output of the MZM. At quadrature, both MZM outputs receive equal amplitudes of each field component. Under null bias, the output of interest contains only odd order components while the other output contains only even order terms. If the two branches of the modulator do not experience equal and opposite phase modulation, the terms will not cancel as predicted. For a MZM with single-arm phase modulation, all terms aside from the carrier are independent of the bias. Zero-chirp MZMs often employ a symmetric electrode design to achieve balance. Even with balanced modulation, the amount of suppression is limited by the degree of balance between the arms of the interferometer. A well-designed modulator can achieve about 30 dB of suppression. Figure 4 shows the OSA spectrum for a MZM biased in a null. This particular MZM is fairly well balanced and achieves an optical carrier suppression of almost 25 dB.

It is both useful and informative to compare the results derived here for the optical field to those derived previously for the RF photocurrent of a microwave photonic link. In [11], for the same applied voltage, the relative strengths of the RF photocurrents was derived as

$$\begin{cases} (\pm 1)^n 2\cos\Gamma_0 J_n\left(\frac{\pi v_1}{V_\pi}\right) J_m\left(\frac{\pi v_2}{V_\pi}\right)\cos\left(n\omega_1 \pm m\omega_2\right)t, \\ \qquad\qquad n+m,\ even \\ -(\pm 1)^{n+1} 2\sin\Gamma_0 J_n\left(\frac{\pi v_1}{V_\pi}\right) J_m\left(\frac{\pi v_2}{V_\pi}\right)\sin\left(n\omega_1 \pm m\omega_2\right)t, \\ \qquad\qquad n+m,\ odd \\ \qquad\qquad n,m = 0,1,2,\ldots \end{cases} . \tag{4}$$

Biasing the modulator at quadrature ($\Gamma_0 = \pi/2$) yields the commonly accepted result of nulling the second order nonlinearity (when $n + m$ is even, $\cos(\Gamma_0) = 0$). Notice the dependence on Γ_0 in (4) as compared to $\Gamma_0/2$ in (3). This is consistent with the fact that second order terms can be present in the optical field but not in the RF photocurrent.

Equation (3) provides the information we need about the optical field to evaluate the channelizer in terms of linearity. The optical filter will route the terms defined by (3) onto the output ports (channels) according to their optical frequency. To determine the RF photocurrent for a particular channel, we must combine the optical local oscillator with the field components that are routed to that channel and calculate the resulting field intensity. Generally speaking, any two components in the optical field separated by ω contribute to the RF term at that frequency. The photodetector, a photon-counting device, responds to the intensity of the optical electric field. We calculate the intensity by squaring the magnitude of the electric field. In doing so, we see that any pair of electric field components separated by ω result in a cross term, or "beat term", which causes the intensity to fluctuate at ω. This is consistent with the classical view of the photodetector as a square-law device for the electric field. In both views, we must consider the contribution of all the pairs of field components whose separation is ω in order to accurately predict the RF photocurrent at ω.

As an example, consider the MZM biased at quadrature under a relatively low modulation depth. We can see from (3) and Fig. 3 that the optical field is significant at $\omega_0 \pm 2\omega_1$, but (4) tells us there is no RF photocurrent at $2\omega_1$. Clearly, each of the upper and lower sideband will beat with the carrier to create time-varying intensity terms at $2\omega_1$. The common assumption is that these two cancel and the resulting RF photocurrent is zero. In fact, these two add together. It is the beat term between the upper and lower fundamentals at $\omega_0 \pm \omega_1$, which are also $2\omega_1$ apart, that cancels the two terms mentioned previously. If we remove the small signal approximation, there are an infinite number of pairs of terms in the optical field that are separated by $2\omega_1$. The vector sum of all of these cross terms gives the RF photocurrent at $2\omega_1$.

It is useful to consider other optical modulators for use with the channelizer. Phase modulators (ΦMs) are not practical for traditional microwave photonic links because the upper and lower sidebands of the signal cancel at the photodetector and no RF photocurrent results. In the channelizer, however, only one of the sidebands is combined with an optical local oscillator, so the cancellation does not occur. The next subsection briefly analyzes the ΦM as a potential modulator for an optical channelizer based on optical filtering.

3.2 Phase Modulator for Use in an Optical Channelizer

For an ideal ΦM, the phase of the input complex exponential is modulated via the electrooptic effect as

$$E_0 e^{j\omega_0 t} e^{j\phi(t)}. \tag{5}$$

Assuming $\phi(t)$ is of the same form as (2), and applying the appropriate Bessel identities to simplify yields an expression for the individual field components,

$$E_0 e^{j\Gamma_0} J_n\left(\frac{\pi v_1}{V_\pi}\right) J_m\left(\frac{\pi v_2}{V_\pi}\right) e^{j(\omega_0 + n\omega_1 + m\omega_2)t}, \quad n, m = \ldots, -1, 0, 1, 2, \ldots \tag{6}$$

which is simpler than (3), but very similar. One important difference lies in the fact that the ΦM is a single path device. Notice both even and odd order terms share the same dependence on the bias, Γ_0, which only affects the overall phase of the components. On the other hand, (3) shows that the amplitudes of the even and odd harmonics depend differently on the bias for a MZM. Thus, the MZM provides a mechanism for controlling the relative amplitudes of the even and odd

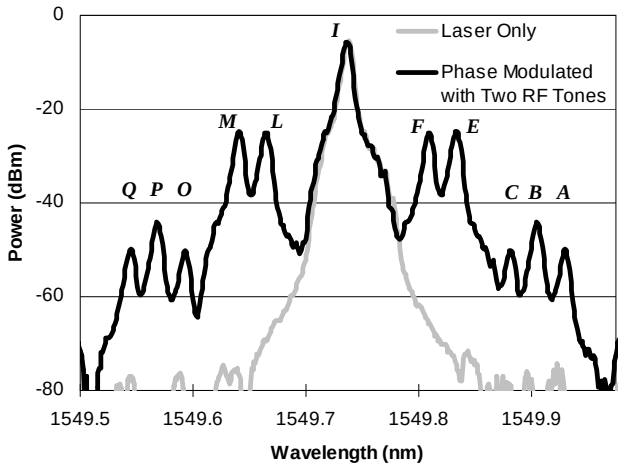

Fig. 5. Optical spectrum analyzer (OSA) plot of a ΦM with two +5 dBm RF tones at 9 GHz and 12 GHz applied. The labels applied to this plot correspond only to the frequencies in Fig. 2 and Table I assuming $\omega_1=2\pi\cdot 9$ GHz and $\omega_2=2\pi\cdot 12$ GHz. The laser-only spectrum illustrates the limitation due to the OSA.

harmonics while the ΦM does not. Figure 5 captures the optical spectrum of a ΦM. Notice how closely this plot resembles Fig. 3. Recall that for a MZM biased at quadrature, the amplitude scaling due to the bias is equal for both even and odd order terms.

The electrooptic effect is known to be quite linear in lithium niobate modulators; hence the phase of the optical signal depends linearly on the applied voltage. This implies that a ΦM and the two branches of a balanced MZM can be modeled as near-perfect phase modulators. Unfortunately, phase modulation is inherently nonlinear in the electric field. In phase modulation the input signal appears as part of the argument of a trigonometric or exponential carrier. Expanding the carrier into a Taylor series readily exposes the unavoidable nonlinearity. The numerous harmonics shown in Fig. 5 illustrate this problem clearly. Ideally, the optical channelizer prefers a modulator that is linear in the optical field.

In terms of RF efficiency, the ΦM outperforms the MZM. Even if the MZM is biased at a null to maximize the fundamental term, the argument of the Bessel function for the ΦM in (6) is twice as large as for the MZM in (3). Unfortunately, the carrier-to-third-order-intermodulation ratio is not improved in the ΦM compared to the MZM.

One frequently overlooked implication of electrooptic (phase-based) modulation is the interdependence of all the components on the total applied voltage. For the two-tone examples derived in (3) and (6) we noticed that the amplitude of each term (including the optical carrier and fundamentals) depends on the drive amplitudes of both tones. Expanding this to multiple tones (or noise) would show that the amplitude of every frequency component in the optical field depends partially on all of the frequency components of the applied voltage. This means that one strong signal can affect all the others. Furthermore, since the problem occurs in the modulator itself, it cannot be solved with filtering. Finally, since both MZM and ΦM use this phase modulation mechanism, both are subject to this phenomenon.

3.3 Electro-Absorption Modulation for Use in an Optical Channelizer

The electro-absorption modulator (EAM) has long been used in digital communications systems owing to its simple integration with semiconductor lasers, small size, and low drive voltage[16],[17]. The typical EAM, however, has a nonlinear response and a limited input power, making it unsuitable for most analog optical applications. Additionally, the response depends heavily on bias, input optical power, and operating wavelength [18]-[20]. As a result, a general

and straightforward analysis is not practical.

Research on EAMs has focused on both increasing the maximum input power and improving the linearity[19],[20]. Since EAMs are not based on the electrooptic effect (phase modulation), electrical pre-distortion for EAMs or specially designed EAM structures could potentially offer linear optical field, but the problem is largely unsolved as yet. In their current state, EAMs are not the best choice for use in an optical channelizer system.

For the optical channelizer, the MZM biased at a null is currently the best option for optical-to-electrical conversion. The spurious-free dynamic range (SFDR) and a host of other performance metrics for MZM-based photonic links have been derived [11]-[15]. Most of these assume the entire optical spectrum is incident on the photodetector and only consider the RF photocurrent defined by (4). For the optical channelizer, however, the impact of nonlinearities should be reconsidered in the context of a MZM biased at null. The next section discusses how these nonlinearities affect the performance of the optical channelizer.

4 IMPACT OF MODULATOR NONLINEARITIES ON AN OPTICAL CHANNELIZER

Assume an ideal non-cyclic optical channelizer filter with infinite out-of-band suppression. In other words, the filter passes only the portion of the spectrum (the channel) designed to exit a particular channel. For two tones applied to a balanced and null-biased MZM, the third-order intermodulation product is the dominant nonlinearity. The $2\omega_1 - \omega_2$ (or $2\omega_2 - \omega_1$) term is particularly bothersome because it falls within the band of a single octave system.

A common linearity metric for analog systems is the two-tone spurious free dynamic range (SFDR) [21]. In a traditional MZM-based link, the strength of the optical carrier relative to the other field components depends only on the drive strength of the input tones and the bias point of the modulator. Furthermore, the entire spectrum reaches the photodetector. Biasing the MZM at quadrature and assuming the shot noise limit, one can calculate the theoretical SFDR as a function of received DC photocurrent [11]. For the optical channelizer, on the other hand, the optical local oscillator (OLO) power is controlled independently of the other field components exiting the MZM. As a result, the SFDR depends on the relative strength of the OLO to the

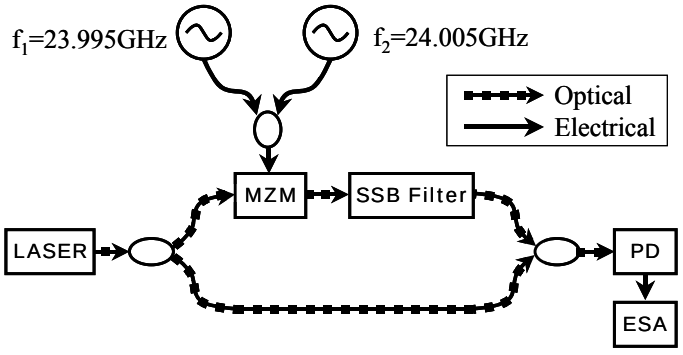

Fig. 6. Experimental setup to emulate an optical channelizer. Mach-Zehnder modulator (MZM) is null-biased. The single sideband (SSB) filter suppresses the carrier and one of the sidebands, selecting a single "channel" of the optical spectrum. The carrier introduced by the laser and suppressed by the MZM and SSB filter is reintroduced as a local oscillator before the photodetector (PD). Measurements are taken at the electrical spectrum analyzer (ESA) as the RF input powers are varied.

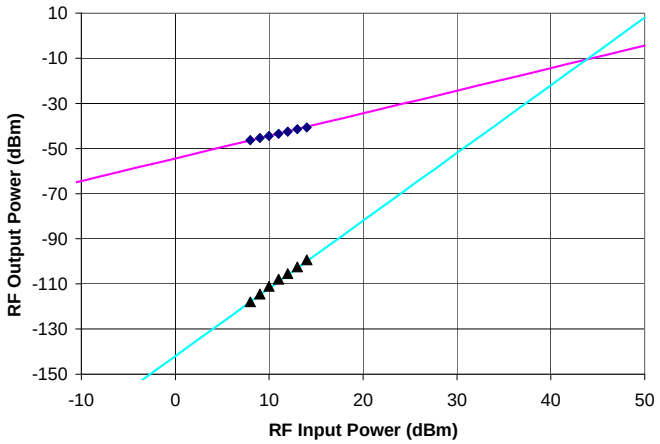

Fig. 7. Two tone spurious-free dynamic range (SFDR) measurement for emulated optical channelizer of Fig. 6. The extrapolated output third-order intercept is –11 dBm. The noise was measured as shot noise limited at 4 mA DC photocurrent through a Discovery DSC30S photodetector for a measured SFDR of 105 dB·Hz$^{2/3}$.

fundamentals. Furthermore, since the spectrum is channelized after modulation, it is entirely possible for the two tones and their intermodulation products to be routed to different output channels. For comparison, one can assume the tones of interest exit the same port of the channelizer filter. Since the MZM limits the linearity in both systems, the carrier-to-intermodulation ratio for the channelizer will equal that of the traditional link. The shot noise, output third-order intercept point and corresponding SFDR, however, depend on the magnitude of the OLO.

We can simulate an optical channelizer with the experimental setup shown in Fig. 6. The single sideband (SSB) filter is actually an ultra-narrow fiber Fabry-Perot filter that passes both fundamentals and the associated third-order spurs created in the modulator. This emulates a single channel for the optical channelizer. The lower branch of the final optical combiner emulates the OLO. The setup is designed for a two-tone spurious-free dynamic range measurement. All of the fiber and couplers were polarization maintaining. The null-biased MZM combined with the SSB optical filter suppressed the optical carrier > 50 dB. The measured MZM-plus-filter insertion loss was 7.5 dB. The measured SFDR data and linear fits for this setup are shown in Fig. 7. Based on the shot-noise-limited noise floor at a received DC photocurrent of 4 mA and an output third-order intercept (OIP3) of –11 dBm, the calculated SFDR is 105 dB·Hz$^{2/3}$.

One of the proposed benefits of an optical channelizer is very large and potentially multi-octave system bandwidth. Even over multiple octaves, the null-biased MZM is limited predominantly by third-order intermodulation, followed by the third harmonic of the fundamentals. Several approaches have been explored to provide highly linear analog optical links. The vast majority of these techniques focus on linearizing the RF photocurrent [22]-[25]. For both MZM and ΦM, the fundamental nonlinearity introduced in the optical field by the electrooptic effect is unavoidable. Additionally, canceling these nonlinearities in the optical domain is currently quite difficult. It remains uncertain whether research on EAMs will result in modulators that are linear in the optical field. For the foreseeable future, the optical modulator will impose linearity limits on this optical channelizer system.

5 SUMMARY AND CONCLUSIONS

Advanced photonic systems such as the optical channelizer are emerging that will assume more and more of the functionality traditionally performed by electronics. The requirements for the components in such systems are much more stringent than those required for simple RF link extension. Section 2 outlined the basic principle of the optical channelizer, a different approach from earlier acousto-optic channelizers. With optical local oscillators and a narrow channel spacing optical filter, the architecture avoids some of the fundamental inefficiencies of previous optical channelization approaches. Compared to an RF channelizer, the optical channelizer performs both channelization and down-conversion in the optical domain. Analysis of the system demands careful consideration of the optical field.

Section 3 presented the optical electric field as a function of applied input voltage for both a ΦM and a MZM. Both modulators depend on the electrooptic effect, but the MZM provides the ability to adjust the relative amplitudes of the even and odd order nonlinearities, provided the MZM is balanced. When biased in a null, the MZM suppresses the even order terms and provides maximum signal-to-optical field efficiency. The RF photocurrent for a given channel then depends only on the optical field components passed by the optical filter – a very different situation in general than the traditional photonic link.

Nonlinearities due to the modulator and their impact on channelizer performance were considered in Section 4. Assuming ideal filters, the performance theoretically approaches that of a MZM-based photonic link, but only when the MZM is null-biased. Furthermore, any imperfections in the channelizer optical filter directly translate to performance penalties.

In terms of linearity, modulators pose the most immediate limitation. The optical channelizer architecture outlined in this work demands advances on several device and subsystem fronts including optical filtering, optical local oscillator generation, and optical modulators that are linear *in the optical field*. Work should be pushed forward on these fronts because the channelization of extremely large RF frequency spectra performed in the optical domain will provide new tools for a wide variety of signal processing applications.

ACKNOWLEDGEMENT

The authors wish to acknowledge technical discussions with Steve Pappert of DARPA and Ron Esman, Terry Turpin, Fred Froehlich, Jim Lafuse, and others at Essex Corporation, Columbia, MD.

REFERENCES

[1] G. W. Anderson, D. C. Webb, A. E. Spezio, and J. N. Lee, "Advanced channelization for RF, microwave, and millimeterwave applications," *Proc. IEEE*, vol. 79, pp. 355-388, Mar. 1991.

[2] J. B. Tsui, "Bragg Cell Receivers (Optical Processors)," Microwave Receivers and Related Components, Los Altos, California: Peninsula, 1985, Chapter 7, pp.149-181.

[3] T. Yumaz, C. M. DePriest, P. J. Delfyett Jr., T. Turpin, J. H. Abeles, and A. Braun, "Modelocked external cavity semiconductor laser for applications in photonic arbitrary waveform generation and photonic synthesis," in *Proc. 15th Annu. Meet. IEEE Lasers and Electro-Optics Society (LEOS 2002)*, vol. 2, pp. 10-14, Nov. 2002.

[4] T. M. Turpin, F. F. Froehlich, and D. B. Nichols, "Optical tapped delay line", US patent 6,608,721, to Essex Corp., 2003.

[5] R. Logan, "All-optical heterodyne RF signal generation using a mode-locked-laser frequency comb: theory and experiments," in *2000 IEEE MTT-S Int. Symp. Dig.*, Boston, MA, June 2000, pp. 1741-1744.
[6] T. Ohno, K. Sato, S. Fukushima, Y. Doi, and Y. Matsuoka, "Application of DBR mode-locked lasers in millimeter-wave fiber-radio system," *J. Lightwave Technol.*, vol. 18, pp. 44-49, Jan. 2000.
[7] A. Kellner, B. Lam, G. Yan, and P. Yu, "Externally modulated mode-locked laser diodes for microwave transmission links," *Electron. Lett.*, vol. 25, pp. 1291-1293, Sept. 1989.
[8] W. Man, P. Andrekson, and J. Toulouse, "Investigation of a spectrally flat multi-wavelength DWDM source based on optical phase- and intensity-modulation," in *2004 Optical Fiber Comm. Tech. Dig.*, Los Angeles, CA, Feb. 2004, paper MF78.
[9] S. Yamashita and G. Cowle, "Bidirectional 10-GHz optical comb generation with an intracavity fiber DFB pumped Brillouin/erbium fiber laser," *IEEE Photon. Technol. Lett.*, vol. 10, pp. 796-798, June 1998.
[10] C. H. Bulmer, and W. K. Burns, "Linear interferometric modulators in Ti:$LiNbO_3$," *J. Lightwave Tech.*, vol. LT-2, pp. 512-521, Aug. 1984.
[11] B. H. Kolner, and D.W. Dolfi, "Intermodulation distortion *OSA J. Applied Optics*, vol. 26, pp. 3676-3680, 1987.
[12] L. T. Nichols, K. J. Williams, and R. D. Esman, "Optimizing the ultrawide-band photonic link," *IEEE Trans. Microwave Theory and Tech.*, vol. 45, pp. 1384-1389, Aug. 1997.
[13] C. H. Cox III, G. E. Betts, and L. M. Johnson, "An analytic and experimental comparison of direct and external modulation in analog fiber-optic links," *IEEE Trans. Microwave Theory and Tech.*, vol. 38, pp. 501-509, May 1990.
[14] E. Ackerman, S. Wanuga, D. Kasemset, A. S. Daryoush, and N. R. Samant, "Maximum dynamic range operation of a microwave external modulation fiber-optic link," *IEEE Trans. Microwave Theory and Tech.*, vol. 41, pp. 1299-1306, Aug. 1993.
[15] S. A. Maas, Nonlinear Microwave Circuits, New York: McGraw-Hill, 1988, pp. 155-207.
[16] S. O'Brein, H. Foulk, H. Gebretsadik, N. Frateschi, W. Choi, A. Bond, S. Robertson, and R. Jambunathan, "Highly integrated 1.55 um analog transmitter for high speed (15 GHz) high dynamic range analog transmission," in *2004 Top. Meet. on Microwave Photon. Tech. Dig.*, Ogunquit, ME, Oct. 2004, pp. 281-284.
[17] S. Kaneko, M. Noda, H. Watanabe, K. Kasahara, and T. Tajime, "An electroabsorption modulator module for digital and analog applications," *J. Lightwave Technol*., vol. 17, pp. 669-676, Apr. 1999.
[18] K. K. Loi, J. H. Hodiak, X. B. Mei, C. W. Tu, and W. S. C. Chang, "Linearization of 1.3um MQW electroabsorption modulators using an all-optical frequency-insensitive technique," *IEEE Photonic Tech. Lett.*, vol. 10, pp. 964-966, July 1998.
[19] B. Liu, J. Shim, Y.-J. Chiu, H. F. Chou, J. Piprek, and J. E. Bowers, "Slope efficiency and dynamic range of traveling-wave multiple-quantum-well electroabsorption modulators," *IEEE Photonic Tech. Lett*., vol. 16, pp. 590-592, Feb. 2004.
[20] R. B. Welstand, C. K. Sun, S. A. Pappert, Y. Z. Liu, J. M. Chen, J. T. Zhu, A. L. Kellner, and P. K. L. Yu, "Enhanced linear dynamic range property of Franz-Keldysh effect waveguide modulator," *IEEE Photonic Tech. Lett.*, vol. 7, pp. 751-753, July 1995.
[21] W. E. Stephens, and T. R. Joseph, "System Characteristics of Direct Modulated and Externally Modulated RF Fiber-Optic Links," *J. Lightwave Technol.,* vol. LT-5, pp. 380-387, Mar. 1987.
[22] A. Katz, W. Jemison, M. Kubak, and J. Dragone, "Improved radio over fiber performance using predistortion linearization," in *2003 IEEE MTT-S Int. Symp. Dig.*, Philadelphia, PA, June 2003, pp. 1403-1406.

[23] T. Ismail, C. Liu, J. Mitchell, and A. Seeds, "Interchannel distortion suppression for broadband wireless over fibre transmission using feed-forward linearised DFB laser," in *2004 Top. Meet. on Microwave Photon. Tech. Dig.*, Ogunquit, ME, Oct. 2004, pp. 229-232.
[24] M. Nazarathy, J. Berger, A. Ley, I. Levi, and Y. Kagan, "Progress in externally modulated AM CATV transmission systems," *J. Lightwave Technol.*, vol. 11, pp. 82-105, Jan. 1993.
[25] P. Myslinski, C. Szubert, A. Freundorfer, P. Shearing, J. Sitch, M. Davies, and J. Lee, "Over 20 GHz MMIC pre/postdistortion circuit for improved dynamic range broadband analog fiber optic link," *Microwave and Opt. Technol. Lett.*, vol. 20, iss. 2, pp. 85-88, Jan. 1999.